ESTIMATION OF HARDNESS IN NICKEL-BASE HARDAFACING DEPOSITS ON 316LN STAINLESS STEEL BY MAGNETIC TECHNIQUES

G. Chakraborty, V. Ramasubbu, S.K. Albert,
A.K. Bhaduri, N. Thirumurugan, A. Bharathi and B. Raj

ABSTRACT

Nickel-base Colmonoy-6 (AWS ERNiCr) alloy is the material chosen for hardfacing of austenitic stainless steel (SS) components used in India's Prototype Fast Breeder Reactor. Gas Tungsten Arc deposited Colmonoy hardfacing alloys suffer from significant loss in hardness and wear properties due to dilution from the austenitic stainless steel substrate. Although both austenitic SS and the undiluted Colmonoy-6 alloy are non-magnetic, the hardfacing deposit diluted by SS becomes ferromagnetic. In a multilayer deposit, magnetism is highest in the first hardfacing layer and decreases progressively in the subsequent layers. As in actual hardfacing deposits, dilution is difficult to control for any deposited layer, it is not easy to study variations of magnetic properties as a function of dilution. Hence, a separate set of deposits (twin-deposits) were produced by co-deposition of Colmonoy-6 alloy rods and austenitic SS filler wire on a copper block. Magnetic properties of hardfacing and twin-deposits were examined using Magnegage and Feritscope equipments. The saturated magnetic moments and Curie temperature of the twin-deposits were measured from room temperature to 873 K. Further, optical, scanning electron microscopy, energy dispersive X-ray spectroscopy and hardness measurements were performed for both hardfacing and twin-deposits. Correlation between hardness, microstructure and bulk magnetic property of deposits with different dilution levels could be established. It was also possible to correlate hardness with the magnetic property of the deposits. Thus, the present study indicates a potential use of magnetic techniques for estimating hardness and dilution of the Colmonoy hardfacing deposit in a component, which cannot be subjected to destructive examination.

IIW-Thesaurus keywords: Dilution; Electromagnetic fields; Energy input; Hardfacing; Hardness.

1 Introduction

Nickel-base Colmonoy (AWS ER NiCr) alloys, offering excellent resistance to wear, corrosion and high temperature properties [1], find extensive application for hardfacing of austenitic stainless steel (SS) components used in sodium-cooled fast breeder reactors operating at temperatures up to 823 K. This alloy replaces more widely used cobalt-base Stellite alloys because of the high induced radioactivity originating from the Co^{60} isotope in Stellites [2]. However, Colmonoy alloys deposited by the GTAW process are affected by a significant dilution by the austenitic SS substrate caused by large differences in the melting temperature range between the substrate and the deposited alloys [3]. Dilution has a significant effect on microstructure, hardness and hence, wear-resistance of the deposit [4, 5]. To overcome the adverse effects of dilution on hardness and wear-resistance of the deposit, the minimum thickness specified for Ni base deposits on hardfaced components is high, which in turn increases the deposited volume and hence the susceptibility of the deposit to shrinkage cracking during deposition due to the associated thermal stresses.

Both Colmonoy alloys and austenitic SS are non-magnetic. However, it is observed that the hardfacing alloy deposits of Colmonoy on austenitic SS substrate exhibit ferromagnetism. The susceptibility to magnetic attraction is highest for the highest level of dilution and reduces with dilution. It is reasonable to assume that magnetism not present in the undiluted deposit but observed in the deposits diluted by the base metal is caused by dilution, which results in an increase in the Fe content in the deposit and makes it essentially a Fe-Ni-Cr alloy. Fe-Ni alloys are magnetic in certain composition ranges, which are popularly known as Invar alloys. It is well-known from magnetization studies in bulk FCC Fe-Ni alloys [6] that with increasing Fe content in the Fe_xNi_{1-x} lattice, the magnetic moment shows a systematic increase and reaches a maximum at $x \approx 0.6$. Thus the increase in magnetization seen in the diluted samples is largely caused by the increase in Fe content.

Doc. IIW-2170, recommended for publication by Commission V "Quality Control and Quality Assurance of Welded Products."

For transition metal alloys containing Fe, the trend in the magnetic moment variation is documented as the Slater-Puling curve which shows a maximum at an electron-to-atom ratio of 26.5. Both the Fe-Ni bcc and fcc alloys fall on this curve, with the magnetic moment increasing with Fe content in the Ni-rich region [7]. The presence of different alloying elements also has a definite action on the observed magnetism in case of Fe-Ni alloys [7-9]. For example, a Cr to Ni addition seems to reduce the magnetic moment of Ni; Mo being iso-electronic to Cr also decreases the magnetic moment of Ni. Secondary effects, viz. lattice parameter changes are also another responsible parameter for high magnetic moments in Fe-Ni alloys. Mo, with its atomic size larger than that of Ni and Fe, is known to alter the lattice parameters of Fe-Ni alloys [8, 9].

In the present study, the origin of magnetism in the diluted deposits is explored. As both hardness and magnetism indicate distinct relations with dilution of the deposits by substrate base materials, an attempt has been made to establish a correlation between hardness and magnetism of the deposits.

In a multilayer deposit by the GTAW process, dilution is highest in the first layer, deposited on the base metal, and dilution decreases progressively in the subsequent layers made on previously deposited layers. It is not possible to control the extent of dilution in different layers and hence, in order to produce hardfacing deposits of known and consistent dilution levels, 4 mm-diameter Colmonoy-6 rods were co-deposited with ER 16-8-2 filler wires (SS) of various diameters on a water-cooled copper block (twin-deposit). The copper block does not melt and the deposit thus formed is of uniform composition and known level of mixing between the hardfacing alloy and stainless steel. Another set of samples was prepared by making multilayer hardfacing deposits of Colmonoy-6 rods on 316LN stainless steel (SS) plate. The microstructure, hardness and magnetic property of the deposits are correlated with the dilution of the deposit by austenitic SS. Hardness of the deposit is correlated with its magnetic property so that non-destructive measurement of the magnetic property of the deposit could be used to predict the hardness of the deposit.

2 Experimental

For making deposits on stainless steel base metal, 4 mm-diameter Colmonoy-6 rods were deposited on 125 mm × 75 mm × 30 mm 316LN SS plates using the GTAW process. The 316LN SS base plate was preheated to 673 K, and after deposition, the deposit was cooled in vermiculite powder. The preheating temperature of 673 K was selected based on recommended minimum preheat temperature for hardfacing of austenitic SS components for Indian Prototype Fast Breeder Reactor so as to reduce cooling rate of the deposit and avoid shrinkage cracking. Separate deposits of Colmonoy-6 (size 100 mm × 15 mm), with the number of layers varying from 1 to 5, were produced on five different 316LN SS base plates, with the second layer deposited over the first layer, third layer over the second layer and so on. For these multi-layer deposits, the interpass temperature was maintained at 673 K so as to ensure identical cooling conditions for all hardfacing deposits. All further investigations, like microstructural examinations, magnetic and hardness measurements, and energy dispersive spectra (EDS) studies were conducted on the top surface of the layer (Figure 1) so as to avoid the mixed zone, where previously deposited layers melted and mixed with subsequently deposited layers and re-solidified.

In order to produce deposits of known and consistent dilution, 4 mm-diameter Colmonoy-6 rods are co-deposited with ER 16-8-2 filler wires of various diameters on a 25 mm-thick water-cooled pure copper plate by the GTAW process. The copper block does not melt, thus producing a weld metal produced by proper mixing of the hardfacing alloy and austenitic SS. Deposits thus produced would be referred here as twin-deposits 1 to 6. For deposits 1 to 5, SS filler wires of diameter 0.8, 1, 1.2, 1.6 and 2 mm, respectively, were used and for deposit 6, two SS filler wires each of diameter 2 mm were used along with Colmonoy rods. Before melting, the weight was measured for Colmonoy rods and individual filler wires and dilution of the hardfacing alloy by SS was estimated (Table 1) from the weight ratio of molten SS to molten Colmonoy-6 in the deposit.

To obtain undiluted deposits, bare Colmonoy-6 rods were melted using the GTAW process deposited on the same 25 mm-thick water-cooled copper plate. The nominal chemical composition of the pure Colmonoy-6 hardfacing deposits and 316LN SS are given in Table 2, and details of welding conditions employed in this study are listed in Table 3.

Specimens of undiluted Colmonoy-6 and different hardfacing and twin-deposits were polished by standard metallography techniques. Microhardness indentations were made on the specimens for identifying locations for metallography before and after etching. Micrographs were taken at two different magnifications of 200X and 500X, and the area fraction of precipitates, their morphology and size distributions etc. were estimated using the ImagePro software from 100 micrographs of each deposit. When viewed under optical microscope, the blocky precipitates were revealed even in the unetched condition, while both the blocky and needle-like precipitates were revealed after etching with Murakami reagent. Hence, the area fraction of total precipitates was estimated by image analysis, and the difference

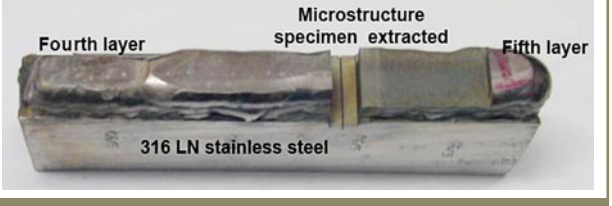

Figure 1 – Colmonoy-6 hardfacing deposit on 316LN stainless steel

Table 1 – Precipitation content and hardness of different deposits

Twin-deposit						Hardfacing deposit				
Deposit no.	% Dilution	% Blocky precipitate	% Total precipitate	% Needle precipitate	Hardness (VHN)	Layer no.	% Blocky precipitate	% Total precipitate	% Needle precipitate	Hardness (VHN)
1	3.93	8.93	17.23	8.3	727	1st	5.09	16.26	11.17	454
2	6.14	7	15.91	8.91	697	2nd	6.88	18.8	11.92	746
3	8.84	6.38	14.61	8.23	619	3rd	7.63	19.65	12.02	810
4	15.72	6.54	13.9	7.36	435	4th	8.02	19.86	11.84	803
5	24.55	5.9	13.28	7.38	380	5th	7.76	19.8	12.04	785
6	49.1	5.63	13.04	7.41	292					

Table 2 – Nominal chemical composition of 316LN stainless steel and Colmonoy-6 [wt. %]

Material	C	Cr	Ni	Mo	Mn	Si	P	S	B	Co	Fe
316LN SS	0.024	17.7	10.8	2.0	1.2	0.4	0.04	0.01	-	0.16	Balance
Colmonoy-6	0.7	14.3	73.75	-	-	4.25	-	-	3.0	-	4.0

Table 3 – Welding conditions used during hardfacing and twin-deposition of Colmonoy-6 and 316LN SS

Welding process	GTAW
Shielding gas	Argon
Shielding gas flow rate	10 $l.min^{-1}$
Arc voltage	13 V
Welding current	100 A
Welding speed	0.8 $mm.s^{-1}$

in the area fraction of the total precipitates and the blocky precipitates gives the area fraction of the needle-like precipitates. As there is a variation in precipitate morphology of the different deposits, the aspect ratio of precipitates was kept fixed for each deposit during image analysis, and the area of precipitates was normalized to a circular morphology in which the size of precipitates is represented as the diameter of the normalized circle.

The metallography samples were further examined under SEM for detailed study about blocky and needle type precipitates. The EDS for the matrix and precipitates in different deposits were also obtained. Assuming that most of the carbon and boron in the alloy are in the precipitates and that the matrix is free from these elements, the approximate composition of the matrix for each layer was estimated from EDS analysis. From the above results, the ratio of Ni/Fe content of the matrix for each specimen is estimated in order to indicate dilution of the sample. Microhardness measurements were performed at 500 g load.

Magnetic measurements on different hardfacing and twin-deposits were carried out using Feritscope and Magnegage. While the Feritscope uses the principle of magnetic induction for measurement, the Magnegage uses the attractive force between a permanent magnet and the specimen. The magnetic field generated by the Feritscope interacts with the magnetic component of the specimen and magnetic dipoles inside the magnetic domains of the specimen are arranged in a preferential direction as a result of external magnetic fields. In contrast, the Magnegage is used mainly for measuring the attractive force produced by weak magnetic fields. Further to be noted, Feritscope gave direct readings whereas for the Magnegage, air reading and white-dial reading were taken for different samples and tearing-off force of the magnet for the sample was estimated from the readings by applying standard formulas. As these instruments are used for estimating the delta-ferrite content in austenitic stainless steel welds and castings, the results obtained are represented as Ferrite Number. However, the term ferrite number can be a misnomer here, as the microstructure of the deposit does not contain any ferritic phase. Hence, in this work, the magnetic property estimated using Magnegage and Feritscope would be referred as Magnegage reading and Feritscope reading, respectively.

For twin-deposit samples, with uniform composition throughout the deposit, the hysteresis loops were generated by recording the magnetic moment in response to variations in applied magnetic fields using a vibrating sample magnetometer at 300 K. The saturation magnetic moments were obtained from the hysteresis loops generated by plotting magnetization against magnetic field. Variation in magnetic moment with temperature in the range of 300-873 K was also determined for twin-deposits at a constant external magnetic field of 500 Gauss. From this, the Curie temperature, above which magnetism disappears, is estimated for each of the deposits. Since dilution is not uniform across the sample for the hardfacing deposits due to the presence of remelted and re-solidified zones, magnetic hysteresis tests were not performed for deposits made on SS plates (hardfacing deposits).

3 Results

Figures 2-4 show optical and scanning electron micrographs of the undiluted Colmonoy-6 and that of different

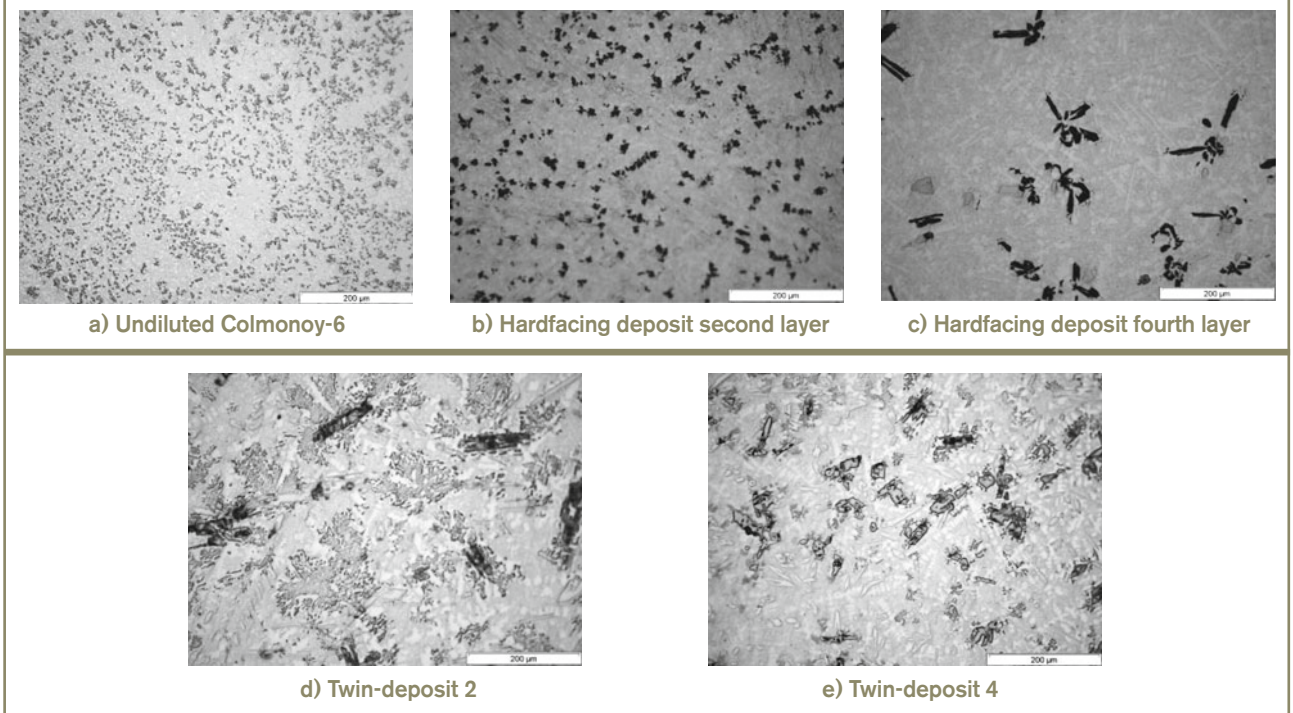

a) Undiluted Colmonoy-6 b) Hardfacing deposit second layer c) Hardfacing deposit fourth layer

d) Twin-deposit 2 e) Twin-deposit 4

Figure 2 – Microstructures of different Colmonoy-6 deposits under unetched condition

hardfacing and twin-deposits. The blocky precipitates are identified as borides and the needle shaped precipitates as carbides [10, 11]. It can be observed that for hardfacing deposits, the size, morphology and distribution of both blocky and needle precipitates vary widely in different layers of the deposit. In the first layer both number and area fraction of the precipitates are small. In the second layer there is an increase in size and area fraction of mainly the boride precipitates. From the third to the fifth layer, morphology and distribution of the borides are similar, with a marginal increase in the size of the precipitates. Less variation in size and volume fraction is observed for carbides than for borides with increasing number of layers or decreasing dilution [12]. For twin-deposits, less variations in morphology and average size of boride precipitates were observed than for hardfacing deposits. The area fraction of blocky and needle-like precipitates estimated by image analysis of optical micrographs of hardfacing and twin-deposits as presented in Table 1 also reflects the higher influence of dilution on area fraction of borides than of carbides.

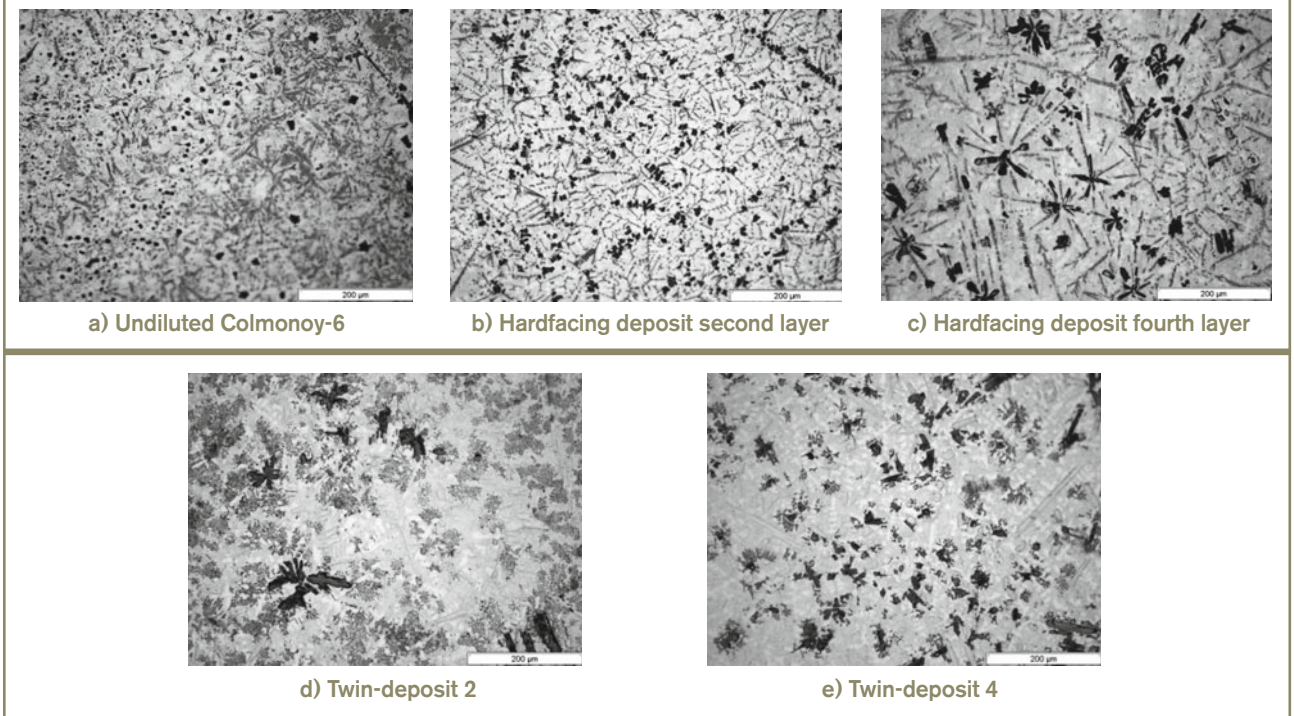

a) Undiluted Colmonoy-6 b) Hardfacing deposit second layer c) Hardfacing deposit fourth layer

d) Twin-deposit 2 e) Twin-deposit 4

Figure 3 – Microstructures of different Colmonoy-6 deposits under etched condition

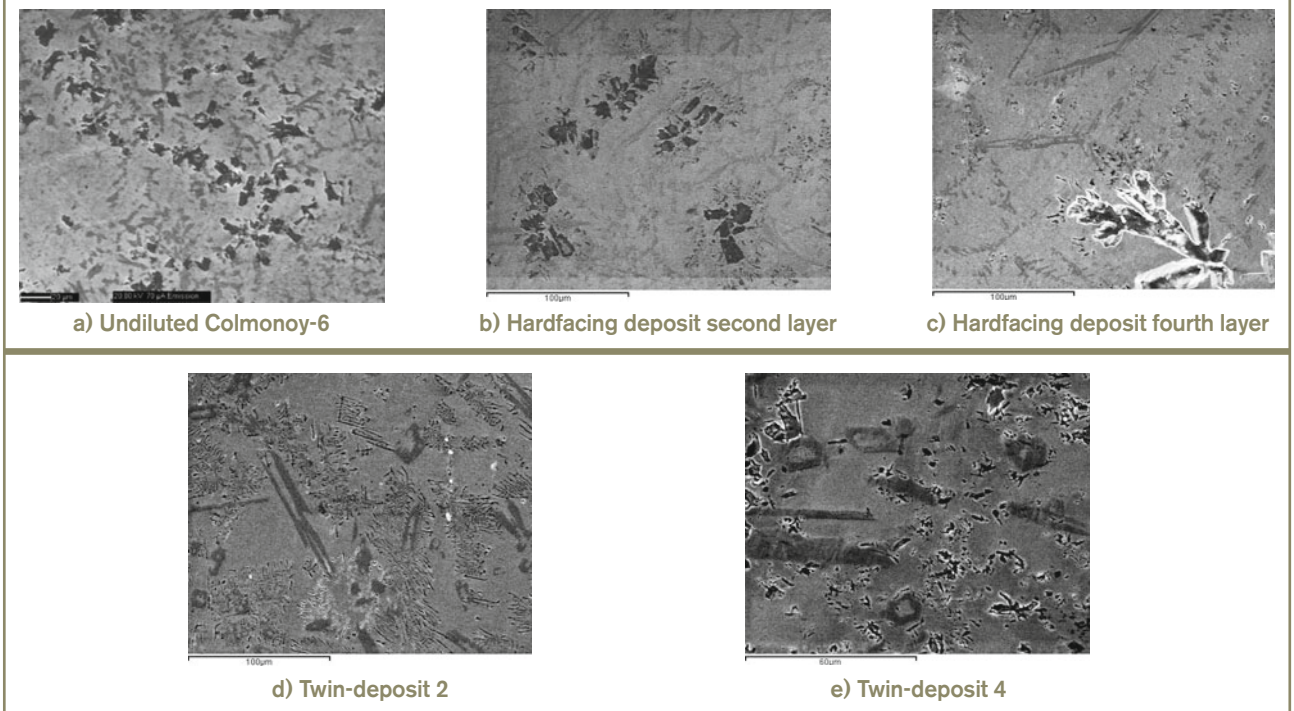

a) Undiluted Colmonoy-6 b) Hardfacing deposit second layer c) Hardfacing deposit fourth layer

d) Twin-deposit 2 e) Twin-deposit 4

Figure 4 – SEM images of different Colmonoy-6 deposits

As the precipitate size is very small and contrast is poor [Figure 2 a)], the area fraction of precipitates could not be estimated in the unetched condition in the undiluted Colmonoy-6 deposits. However, on etching the contrast improved [Figure 3 a)] and the area fraction of total precipitates could be estimated by image analysis to be about 15 %.

It is clear from Table 1 that hardness of the first layer of hardfacing deposits with maximum dilution is quite low compared to that of the undiluted deposits (716 VHN). In the second layer, with decrease in dilution, hardness improves substantially and variation is almost negligible from the third layer onwards. Similarly for twin-deposits hardness improves with decreasing dilution and reaches saturation for low-dilution deposits. It is interesting to note here that the hardness of the undiluted Colmonoy deposited on copper plate is lower than that of the second and subsequent layers of hardfacing deposits and twin-deposit 1. This could be due to low precipitate content (about 15 %) in undiluted Colmonoy-6.

The EDS analyses (Figure 5) of the matrix for the hardfacing, twin and undiluted deposits indicate high iron content and low nickel content at high dilution levels, i.e. in the first layer of hardfacing deposits and twin-deposit 6 as compared to that of undiluted Colmonoy-6. As dilution decreases, the nickel content in the deposit increases for both hardfacing and twin-deposits. It can also be noted (Table 4) that the first layer of hardfacing deposits and all twin-deposits contain molybdenum, an element that is absent in Colmonoy-6 alloy but present only in the 316LN SS substrate material. Further, in twin-deposits, the molybdenum content increased from 0.23 to 0.75 wt. % with increasing austenitic SS (ER 16-8-2 filler wire) content in the twin-deposit.

Table 5 shows the Feritscope and Magnegage readings obtained for both hardfacing and twin-deposits. It is clear that magnetism of the deposit increases with increasing dilution. Having established that the deposit is ferromagnetic and dilution of the deposit by the austenitic stainless steel is the cause of the ferromagnetism observed, saturation magnetic moments were estimated for twin-deposits at 300 K using vibrating sample magnetometer. Induced magnetization vs. magnetic field hysteresis loops for the twin-deposits at room temperature are presented in Figure 6. It can be observed that for deposits 5 and

Table 4 – Variations in matrix composition estimated from EDS analysis of undiluted Colmonoy-6 and different deposits [wt. %]

Element	Twin-deposits						Hardfacing deposits					Colmonoy-6
	1	2	3	4	5	6	1st	2nd	3rd	4th	5th	
Ni	82.46	80.6	75.5	74.4	68.06	62.63	58.78	80.22	83.67	83.67	83.48	83.47
Fe	7.97	10.1	13.68	15.8	20.33	24.4	21.2	9.46	6.31	5.88	4.82	4.83
Cr	4.58	4.4	5.83	5.05	6.88	8.66	16.2	6.35	5.67	6.43	6.63	8.01
Si	4.76	4.44	4.53	4.1	4.1	3.56	2.82	3.97	4.4	4.02	4.63	3.69
Mo	0.23	0.45	0.46	0.6	0.63	0.75	0.99	-	-	-	-	-

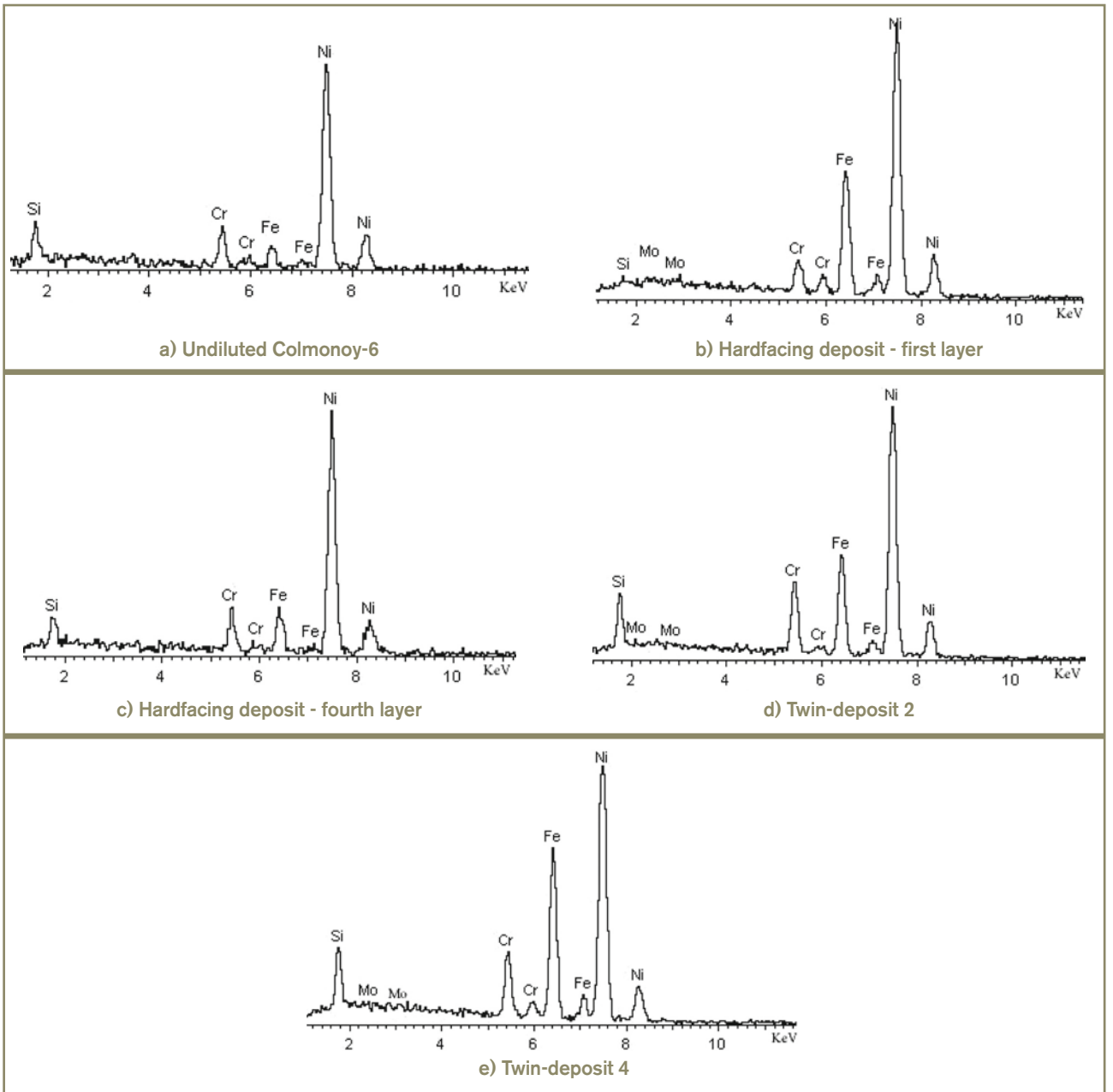

Figure 5 – EDS results, keV vs. Intensity (counts), of different Colmonoy-6 deposits

6, for which dilution is highest, the saturated magnetization is about 40 emu/g; it decreases to 26.6 emu/g for deposit 4, and for deposit 1, with minimum dilution from austenitic SS, this value is only 7.2 emu/g.

In order to study the stability of magnetization of the twin-deposits at high temperature, variations in magnetic moment with increasing temperature in the range of 300-873 K (Figure 7) were determined at constant magnetic field. It can be observed from Figure 7 that except for twin-deposit 3 all other samples follow a similar trend, i.e. for a given temperature magnetic moment is higher for a deposit of higher dilution. The reason for the discrepancy in behaviour of twin-deposit 3 is not clearly known from

Table 5 – Feritscope and Magnegage readings for different deposits

Deposit no.	Feritscope reading	Magnegage reading	Layer	Feritscope reading	Magnegage reading
1	40.1	13.24	First	110	20.72
2	61.4	17.79	Second	30.5	18.15
3	88.4	17.98	Third	4.75	3.91
4	92.64	18.5	Fourth	2.24	2.71
5	116.17	19.1	Fifth	0.99	0.03
6	146.3	19.3			

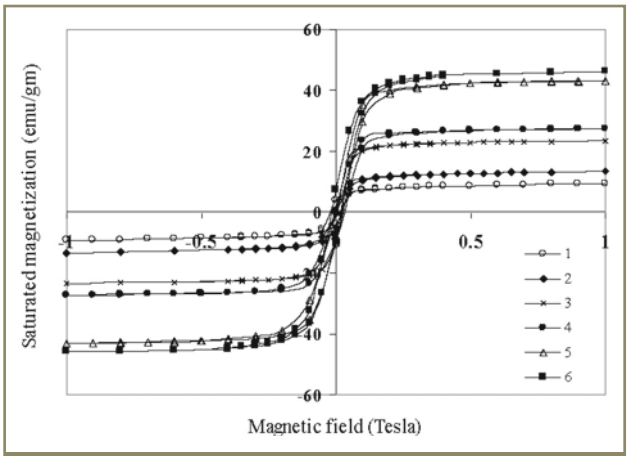

Figure 6 – Variations in saturated magnetization with applied magnetic field for twin-deposits

the present study. In addition to magnetic moment, the Curie temperature is also found to increase with increasing dilution. For deposits 5 and 6, this temperature is about 480 K, and it decreases with decreasing dilution. For deposits 1 and 2, the Curie temperature is about 350 K. This indicates that high-dilution deposits are strongly ferromagnetic with a moderately high Curie temperature.

4 Discussions

The results presented above clearly confirm that dilution from the austenitic stainless steel substrate significantly affects the microstructure and properties of the deposit. It alters the volume fraction, size, morphology and distribution of precipitates in the matrix. For both hardfacing and twin-deposits, there is a clear decrease in the boride content with increasing dilution. In contrast, the corresponding variation for carbides is only marginal. However, cooling conditions of twin-deposits being different from those of hardfacing deposits, less variation in precipitate size is observed for different dilution levels of twin-deposits. It is important to note that not only the matrix composition, but also the precipitate composition is altered by dilution. As both types of precipitates are essentially primary precipitates (formed from the liquid metal during solidification),

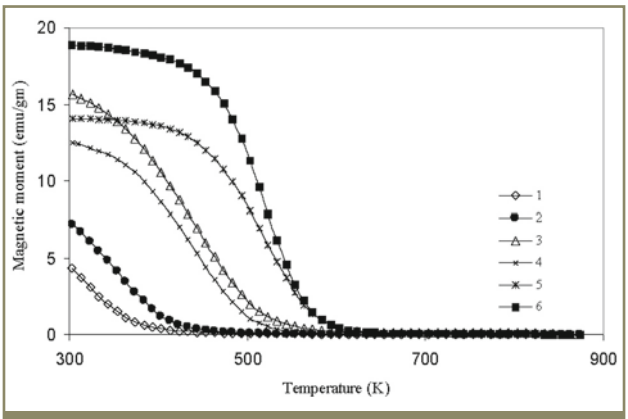

Figure 7 – Variations in magnetic moment with temperature for twin-deposits

it is reasonable to assume that composition changes in the molten metal caused by the dilution is affecting the nucleation and growth kinetics of the precipitates. Further, dilution increases Cr, the major element present in both borides and carbides, in the melt; it can alter the types of borides (CrB, Cr_2B) or carbides (M_7C_3, M_6C or $M_{23}C_6$) formed from the melt [10, 11]. The variation in morphology and composition of precipitates from layer to layer has a significant effect on the hardness of the deposit. Hardness of Cr borides being much higher (2400-2500 VHN) than that of Cr carbides (1000-1200 VHN) [13] and volume fraction of boride precipitates varying more distinctly than carbides with dilution for both hardfacing and twin-deposits, probably explains the wide variation in hardness observed for different hardfacing and twin-deposits.

Results also confirm that magnetic properties observed in the deposits are also associated with dilution. In hardfacing deposits, dilution of the deposit is highest in the first layer and negligible from the third layer onwards; accordingly, magnetic properties are significant only in the first two deposit layers. Thus, magnetism observed both in the hardfacing and twin-deposits is caused by the high Fe content in the alloy due to dilution from the substrate. This is also in agreement with almost no magnetism observed in the third, fourth and fifth deposit layers of hardfacing deposits, with no significant change in Fe content from that of the undiluted deposits.

Though the results indicate that the magnetism observed in the deposits is caused by dilution, the origin of magnetism needs to be explained. Apart from the substitution of Ni atoms by Fe in the Fe-Ni lattice caused by dilution [6, 7], the lattice parameter effect due to Mo [8, 9] is also responsible for ferromagnetization in the diluted deposits. In this context, it is important to note that the highest content of Mo is present in twin-deposit 6, which shows the highest readings for Feritscope, Magnegage and saturated magnetization. However, the origin of magnetism cannot be attributed to changes in lattice parameters caused by the presence of Mo alone in the diluted zone. In case of hardfacing deposits, magnetism is observed even in the second deposit layer, which does not contain any significant amount of Mo. Experimental measurements of lattice parameter variation with dilution of the weld samples would throw light on this issue, although being a multiphase alloy; results may not lead to unambiguous conclusions [14].

Variations in magnetic properties as determined from Feritscope and Magnegage readings for hardfacing deposits as well as twin-deposits [Figures 8 a) and 8 b)] show a fair correlation with the Ni/Fe content of the matrix, with the correlation being better for the former (correlation coefficient: 0.9793) than the latter (correlation coefficient: 0.969). Good correlation obtained for both Feritscope and Magnegage readings with the Ni/Fe ratio indicate that Feritscope and Magnegage, instruments normally used for measuring delta-ferrite contents in stainless steel [15, 16] can be used for estimating the Ni/Fe ratio of the matrix, which is an indication of dilution

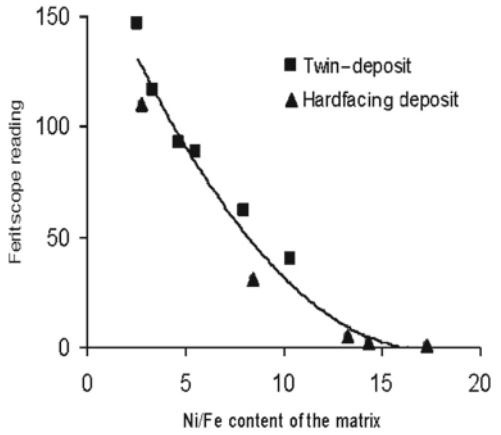

a) in Feritscope reading

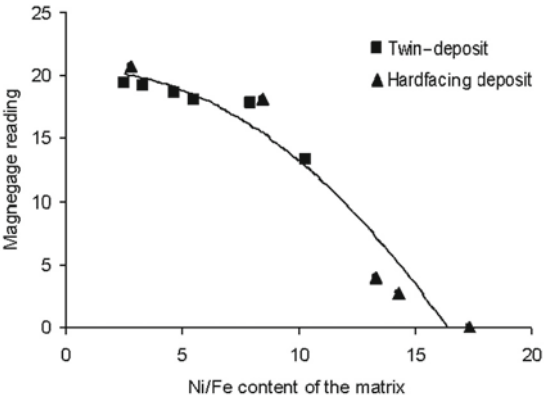

b) in Magnegage reading

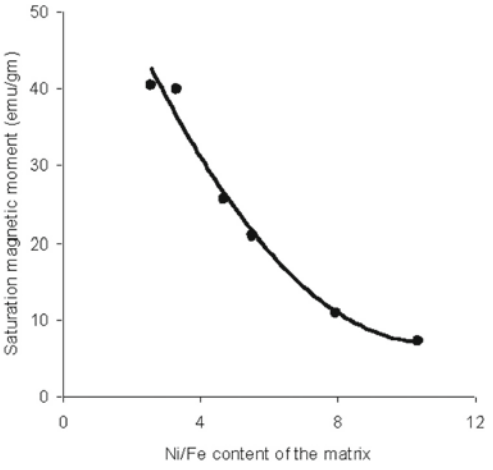

c) in saturated magnetization

Figure 8 – Variations with Ni/Fe content of the matrix of different deposits

of the deposit. Further, for twin-deposits, a good correspondence [Figure 8 c)] is also obtained for saturated magnetization against Ni/Fe ratio (correlation coefficient: 0.9896). Figure 9 a) presents a plot for Ni/Fe ratio against dilution of the matrix as measured by weight ratio of molten SS filler wire to molten Colmonoy alloy for twin-deposits and Figure 9 b) indicates a strong relationship between Curie temperature and hardness with dilution of twin-deposits. Hence, in case of hardfacing of n components, where dilution is difficult to estimate; the magnetic properties measured using Feritscope/Magnegage can be unambiguously used to have an assessment of the dilution of the deposit by the substrate (Figure 10).

As the hardness of the deposits is affected predominantly by the volume fraction of the precipitates and magnetic properties by the composition of the matrix, there is no direct relation between hardness and magnetic properties. However, both are affected by dilution and hence an indirect correlation exists between hardness and magnetic

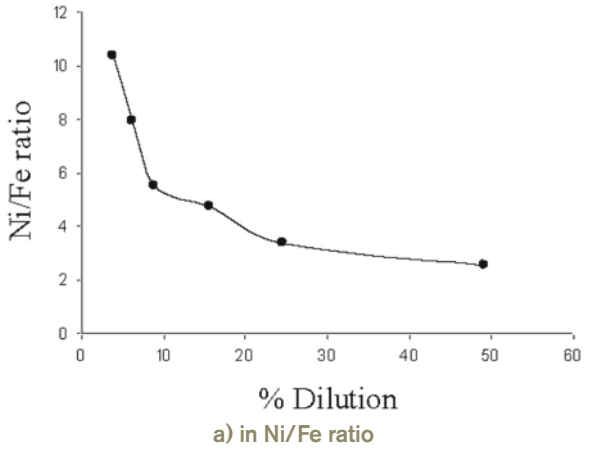

a) in Ni/Fe ratio

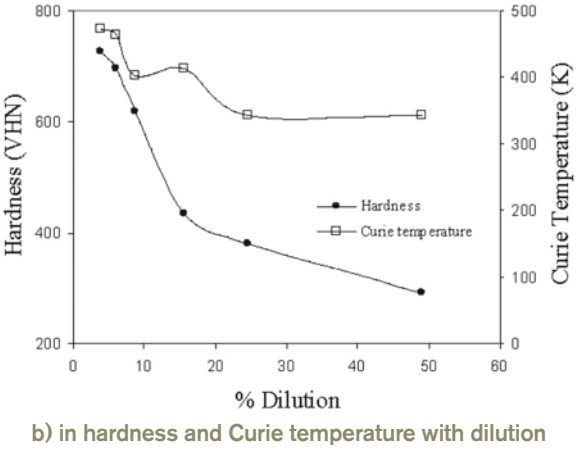

b) in hardness and Curie temperature with dilution

Figure 9 – Variations for different twin-deposits

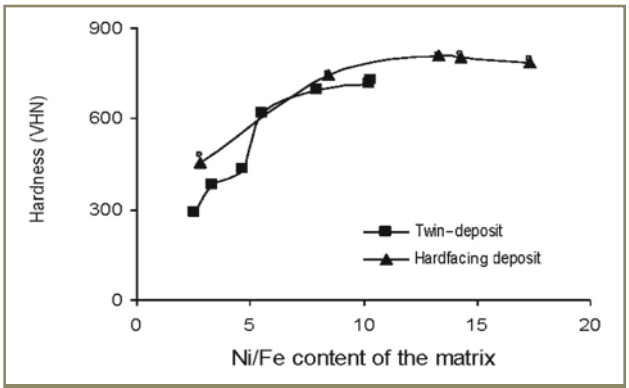

Figure 10 – Variations in hardness with Ni/Fe content of the matrix of different deposits

properties (Figure 11). Hence, one of the potential applications of the results presented here can be the use of magnetic measurements as a non-destructive tool to estimate the surface hardness of Ni-base hardfacing coatings on austenitic stainless steels. Hence, it should be possible to predict the hardness of the deposit simply by measuring the magnetic properties of the deposit by Feritscope and Magnegage. The importance of such measurements is significant in hardfacing of actual components for various applications, which are not suited for in-situ hardness measurements.

5 Conclusions

The major conclusions from the present study on Ni-base Colmonoy-6 hardfacing deposit are the following.

1. Dilution of Ni-base hardfacing deposits by austenitic stainless steel substrates affects not only its hardness but also the magnetic properties of the deposit.
2. Estimation of magnetic moments for twin-deposits at room temperature and high temperatures supports results obtained by Feritscope and Magnegage techniques. A good correlation could be established between the magnetic properties estimated from Feritscope and Magnegage equipments and saturated magnetic moment obtained from magnetic hysteresis loops, with dilution for hardfacing deposits as well as different twin-deposits.
3. The magnetic properties of deposits could also be correlated to their hardness and hence, it is possible to use the magnetic properties of the deposits to predict their hardness and apply this principle to estimate the hardness of deposits on finished components as a non-destructive technique.

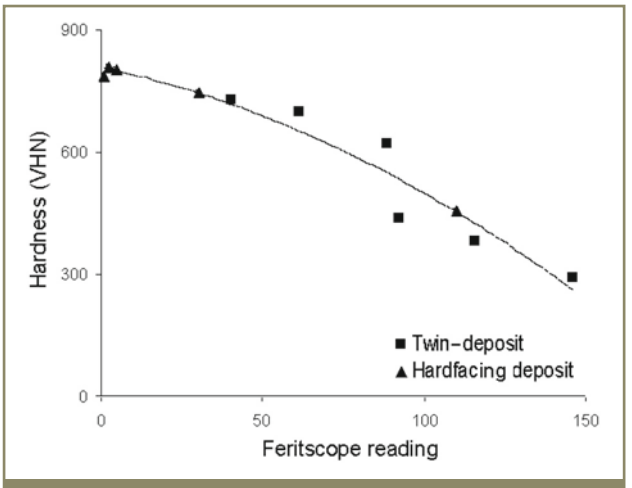

Figure 11 – Variations in hardness with Feritscope reading of different deposits

References

[1] Ohriner E.K., Wada T., Whelan E.P. and Ocken H.: The chemistry, structure of wear resistant, iron-base hardfacing alloy, Metallurgical and Materials Transactions A, vol. 22, no. 5, 1991, pp. 983-991.

[2] Ocken H.: Reducing the cobalt inventory in light water reactor, Nuclear Technology, vol. 68, no. 1, 1985, pp. 18-28.

[3] Davis J.R.: ASM Speciality Handbook of Stainless Steels, ASM International, Materials Park, OH, 1996, p. 10.

[4] ASM Metals Handbook, vol. 6, 9th ed., ASM International, Materials Park, OH, USA, 1993, pp. 794-795.

[5] Rigney D.A.: The roles of hardness in the sliding behavior of material, Wear, 1994, vol. 175, no. 1-2, pp. 63-69.

[6] O'Handley R.C.: in: Modern Magnetic materials: Principals and Applications, John Wiley & sons, 2000, p. 369.

[7] O'Handley R.C.: in: Modern Magnetic materials: Principals and Applications, John Wiley & sons, 2000, p. 145.

[8] Shin J.-C., Doh J.-M., Yoon J.-K., Lee D.-Y. and Kim J.-S.: Effect of molybdenum on the microstructure and wear resistance of cobalt based Stellite hardfacing alloys, Surface and Coatings Technology, 2003, vol. 166, no. 2-3, pp. 117-126.

[9] Hou Q.Y., Huang Z.Y., Shi N. and Gao J.S.: Effects of molybdenum on the microstructure and wear resistance of nickel-based hardfacing alloys investigated using Rietveld method, Journal of Materials Processing Technology, 2009, vol. 209, no. 6, pp. 2767-2772.

[10] Qiang Li, Dawei Zhang, Tingquan Lei, Chuanzhong Chen and Wenzhe Chen: Comparison of laser-clad and furnace-melted Ni-based alloy microstructures, Surface and Coatings Technology, 2001, vol. 137, no. 2-3, pp. 122-135.

[11] Navas C., Colaco R., de Damborenea J. and Vilar R.: Abrasive wear behaviour of laser clad and flame sprayed melted NiCrBSi coatings, Surface and Coatings Technology, 2006, vol. 200, no. 24, pp. 6854-6862.

[12] Ramasubbu V., Chakraborty Gopa, Albert S.K. and Bhaduri A.K.: Effect of dilution on GTAW Colmonoy 6 (AWS NiCr-C) hardfaced deposit made on 316LN stainless steel, Materials Science and Technology, 2011, vol. 27, no. 2, pp. 573-580.

[13] Das C.R., Albert S.K., Bhaduri A.K. and Nithya R.: Effects of dilution on microstructure and wear behaviour of NiCr hardface deposits, Materials Science and Technology, 2007, vol. 23, no. 7, pp. 771-779.

[14] Chakraborty G., Ramasubbu V., Albert S.K., Bhaduri A.K. and Raj B.: Study of magnetism in Colmonoy-6 (AWS NiCr-C) deposit on 316LN stainless steel, Materials Science and Engineering B, 2010, vol. 170. no. 1-3, pp. 133-138.

[15] San Marchi C., Somerday B.P., Tang X. and Schiroky G.H.: Effects of alloy composition and strain hardening on tensile fracture of hydrogen-precharged type 316 stainless steels, International Journal of Hydrogen Energy, 2008, vol. 33, no. 2, pp. 889-904.

[16] Shankar V., Gill T.P.S., Mannan S.L. and Sundaresan S.: Effect of nitrogen addition on microstructure and fusion zone cracking in type 316L stainless steel weld metals, Materials Science and Engineering A, 2003, vol. 343, no. 1-2, pp. 170-181.

About the authors

Dr. Gopa CHAKRABORTY (gopa_mjs@igcar.gov.in), Mr. Velayutham RAMASUBBU (vrsubbu@igcar.gov.in), Dr. Shaju Kattukaram ALBERT (shaju@igcar.gov.in), Dr. Arun Kumar BHADURI (bhaduri@igcar.gov.in), Mr. Natarajan THIRUMURUGAN (nthiru@igcar.gov.in), Dr. Arunachalam BHARATHI (bharathi@igcar.gov.in) and Dr. Baldev RAJ (baldev.dr@gmail.com) are all with Indira Gandhi Centre for Atomic Research, Kalpakkam (India).